SpaceOps-2025, ID # 429

TOWARDS LUNANET LUNAR AUGMENTED NAVIGATION SERVICE (LANS) INTEROPERABILITY DEMONSTRATION AND MONITORING

Cheryl Gramling[a]*, Juan Crenshaw[a], Masaya Murata[b], Richard Swinden[c], Floor Melman[c], Cosimo Stallo [c], Javier Ventura-Traveset[c]

[a] *National Aeronautics and Space Administration (NASA)*, *United States of America, cheryl.j.gramling@nasa.gov**, *juan.m.crenshaw@nasa.gov*
[b] *Japan Aerospace Exploration Agency (JAXA), Japan*, *murata.masaya@jaxa.jp*
[c] *European Space Agency (ESA), Netherlands*, *Richard.Swinden@esa.int, Floor.Melman@ext.esa.int, Cosimo.Stallo@esa.int, Javier.Ventura-Traveset@esa.int*
* Corresponding Author

Abstract

The LunaNet is a lunar communications and position, navigation, and timing (PNT) framework that promotes the use of standards for interoperability among future service providers for lunar missions. NASA, ESA, and JAXA are partnering to develop the LunaNet Interoperability Specification (LNIS), including Applicable Document-1 Volume A defining the Signal in Space features for the Augmented Forward Signal (AFS), which are currently available online. Among the LunaNet PNT services described in the LNIS, the amalgamation of AFS from the service providers will form the Lunar Augmented Navigation Service (LANS) as a multi-laterally coordinated, lunar-focused radio navigation satellite system for upcoming lunar users such as crew, rovers, landers, science instruments, and orbiters. Given that LANS will consist of a minimum of four AFS transmitted in the direction of the Moon, there is a need for in-situ evaluation of performance against the LNIS and to provide assurance that the service enables safe and robust navigation of assets for human and robotic spaceflight operations. Toward achieving the critical objective for safe navigation, JAXA, ESA, and NASA are examining a joint LANS interoperability demonstration mission targeted for the 2028-2029 time frame. Following a description of LunaNet, AFS, and LANS, this paper will provide the mission concept, plans, and objectives for the joint LANS demonstration.

Keywords: Lunar, PNT, AFS, LANS, LunaNet, Interoperability

Acronyms/Abbreviations

AFS	Augmented Forward Signal
C/N0	Carrier to Noise ratio
EIRP	Effective Isotropic Radiated Power
ELFO	Elliptical Lunar Frozen Orbit
ESA	European Space Agency
GNSS	Global Navigation Satellite Service
ICRF	International Celestial Reference Frame
JAXA	Japan Aerospace Exploration Agency
LANS	Lunar Augmented Navigation Service
LCRNS	Lunar Communications Relay and Navigation System
LCNS	Lunar Communication and Navigation System
LNIS	LunaNet Interoperability Specification
LNSS	Lunar Navigation Satellite System
LRR	Laser Retro Reflector
n/a	Not Available
NASA	National Aeronautics and Space Administration
PNT	Position, Navigation, and Timing
PVT	Position, Velocity, and Time
RNSS	Radio Navigation Satellite Service
SISE	Signal in Space Error
UEE	User Equipment Error
UERE	User Equipment Ranging Error
UERRE	User Equipment Range Rate Error

URE User Ranging Error

1. Introduction

Future lunar exploration and science mission plans include operations in areas not in view of Earth and require real time knowledge of their position, velocity, and time. The LunaNet framework defines a set of cooperating networks designed to provide robust and interoperable lunar communications and position, navigation, and timing (PNT) services to the lunar user mission set. This framework is publicly available. For PNT, the imperative is to establish common safe operations in the cislunar/lunar environment.

1.1 LunaNet and the LunaNet Interoperability Specification

In the spirit of the Artemis accords and through mutual study agreements, the National Aeronautics and Space Administration (NASA), European Space Agency (ESA), and Japan Aerospace Exploration Agency (JAXA) are collaborating to define the LunaNet Interoperability Specification (LNIS), which sets standards for the services planned from the associated lunar infrastructure. These standards are critical for ensuring that various lunar services, providers, and technologies can work together effectively. Establishing these international interoperability standards facilitates a more distributed approach to the buildup of critical lunar infrastructure, allowing various service providers to deliver specific services, coverage, and capabilities as demand grows.

The goal is to enable any potential LunaNet Service Provider (LNSP) to implement selected services as defined in the LNIS and achieve seamless integration with the greater LunaNet and service user ecosystem. Among the first service providers to instantiate LunaNet will be NASA's Lunar Communications Relay and Navigation Systems (LCRNS), ESA's Moonlight Lunar Communications and Navigation System (LCNS), and Japan's Lunar Navigation Satellite System (LNSS). This paper covers an in-situ demonstration of interoperability for the Lunar Augmented Navigation Service (LANS), which is instantiated by multiple LNSPs that broadcast the S-band Augmented Forward Signal (AFS). The AFS offers a PNT service as defined in released version 5 of the LNIS [1] and the accompanying Applicable Document-1 Volume A [2]. Following a brief description of the service and providers in section 1, section 2 elaborates on the demonstration objectives. Sections 3, 4, 5, and 6 describe the demonstration architecture, assumptions, planned payload, and operations concept, respectively. Section 7 provides a preliminary performance assessment toward the objectives, and the last section highlights planned future activities among the three cooperating Agencies.

1.2 Augmented Forward Signal (AFS)/Lunar Augmented Navigation Service (LANS)

The LANS represents a key component of LunaNet as described in the LNIS, that defines a Radio Navigation Satellite Service (RNSS) via transmitting the AFS as a broadcast offering. An individual LNSP with multiple geometrically separated nodes can sufficiently deliver services for a mission according to requirements for that LNSP. However, joint LNSP cooperation for LANS may improve individual LNSP capabilities by integrating LNSP asset sources from multiple parties. This concept is illustrated in Fig. 1, where different LNSPs work together to enhance coverage, and improve geometry and user performance.

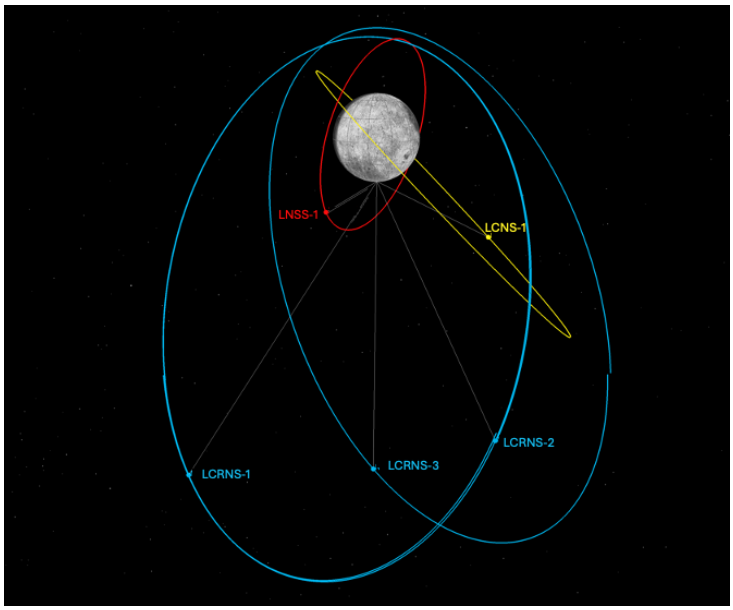

Fig. 1 Lunar position, navigation, and timing services jointly provided by international LNSPs (ESA's LCNS, NASA's LCRNS, and Japan's LNSS). This figure represents the situation in 2029 during the LANS interoperability demonstration in the International Celestial Reference Frame (ICRF). Note that the orbits are notional and are further defined in Table 1.

To achieve LANS interoperability, the LunaNet specifications must consider the challenges associated with different contributing networks operating in the lunar regime. This involves differing orbital designs, with an LNSP possibly using Elliptical Lunar Frozen Orbits (ELFO) to improve availability of these services at the lunar South Pole, while others might opt for circular orbits. Unlike Earth GNSS, this leads to a significant dynamic range amongst received power on the surface, effecting co-channel interference. Besides LNIS Applicable Document-1 Volume A [2], more detail concerning the AFS can be found in existing literature [3][4]. Interoperable participation in LANS implies the service provider adheres to the LNIS.

To ensure the interoperability among different LNSP providers the establishment of a rigorous protocol to access the 4D reference system in which the navigation message is distributed is required. Among the most critical elements, the definition of a lunar reference system (and its materialization, i.e., its associated frame) recognized as international standard and of an international infrastructure tasked with the realization of the time-dependent offset between UTC and a lunar reference time are outstanding.

Three main reference systems are convenient for operations in the cislunar environment: the Lunar Celestial Reference System (LCRS), i.e. the Moon-centered inertial reference system adopted by the International Astronomical Union (IAU) in the IAU Resolution II of 2024 [5]; the Principal Axis (PA) system, i.e. the body-fixed reference system in which aligns with the moments of inertia; and the Mean Earth (ME) system, defined by an X-axis aligned to the Mean-Earth direction and a Z-axis pointing toward the mean rotation axis direction.

Furthermore, radio navigation systems rely on accurate, precise, and continuous time as a reference source for their transmitted signals and messages. GNSS in orbit around Earth act as sources of the Coordinated Universal Time (UTC) timescale reference to Earth's surface of equipotential, the geoid. Even though each system may include an identified offset to UTC, they have consistent clock rates as a fundamental aspect for interoperability. LNSPs providing LANS will disseminate LunaNet Reference Time (LRT) which serves as a reference for the AFS signal. LRT will be traced to UTC [6][7]. The link between LRT and the defined lunar time scale will be defined in future versions of the LNIS.

1.3 LunaNet Service Provider (LNSP) Descriptions

LNSS, LCNS, and LCRNS will be among the first service providers to instantiate LunaNet to enable lunar precise, autonomous landings and surface mobility, while facilitating high-speed, low-latency communication and data transfer between Earth and the Moon. While each system has its own set of requirements that expand upon interoperability specification, they intend to perform as a network of networks. A brief description of each system at the time of the planned demonstration follows.

1.3.1 Japan's Lunar Navigation Satellite System (LNSS)

LNSS is a Japanese lunar PNT system under development, aiming to provide a high-accuracy positioning and navigation service at the lunar South Pole region. The first LNSS satellite is expected to be launched in the 2028-2029 timeframe and its fundamental technologies, such as the GNSS weak signal navigation and the onboard navigation signal generation and broadcasting, will be demonstrated in the lunar environment. The baseline satellite constellation is composed of eight navigation satellites to be deployed in two stable orbits called the Elliptical Lunar Frozen Orbits (ELFOs) [6][7]. The actual satellite orbits and the total number of satellites are subject to change, as the system development proceeds. LNSS complies with the LNIS to become interoperable with the other LNSP and together forms the LANS by broadcasting the AFS towards lunar users. By the time of the demonstration, Japan expects to have one LNSS demonstration satellite deployed in circular lunar polar orbit, transmitting only the AFS.

1.3.2 ESA's Moonlight Lunar Communication Navigation Service (LCNS)

ESA is currently developing the Moonlight Lunar Communications and Navigation System (LCNS), consisting of five satellites − four for navigation and one for communications. These connect to Earth via three dedicated ground stations, creating a data network spanning up to 400,000 km. ESA's lunar communication and navigation infrastructure implementation will occur in phases, beginning with the Lunar Pathfinder, an S-band communications relay satellite manufactured by Surrey Satellite Technology Ltd (SSTL), which is set to begin operations in 2026. Following Lunar Pathfinder, Moonlight LCNS services will be gradually deployed, with initial operations expected by the end of 2028 (Initial Operations Capability (IOC)) and full operations by 2030 (FOC (Full Operations Capability)). By the time of the demonstration, ESA expects to have one LCNS navigation satellite and one LCNS communication satellite in their operational ELFO along with Lunar Pathfinder.

1.3.3 NASA's Lunar Communications Relay and Navigation System (LCRNS)

LCRNS is a NASA Space Communications and Navigation (SCaN) Project within the Goddard Space Flight Center [5]. LCRNS works with, and supports the relay-based communication and PNT (C&PNT) needs of NASA lunar mission stakeholders, including the varied mission set within the Moon-to-Mars (M2M) Artemis Program. The LCRNS Project defines and validates requirements for commercial services that enable an interoperable lunar orbiting C&PNT infrastructure. The LCRNS relay services respond to a three-phased deployment that meets NASA's evolving C&PNT needs in the lunar South Pole Service Volume. Initial Operating Capability-Charlie (IOC-C) requires a minimum of four AFS links in view meeting a Geometric Dilution of Precision (GDOP) less than six for 40% of an Earth day. Each LCRNS AFS must meet a position Signal in Space Error ($SISE_{pos}$) of 13.43m, 3 σ , Commercial services like LCRNS represent a sustainable, long-term approach to human and robotic exploration C&PNT infrastructure, and an extensible solution that meets M2M objectives. By the time of the demonstration, NASA expects to have three AFS transmitters from different lunar orbital nodes that will also provide communication services.

2. LANS Interoperability Demonstration Objectives and Goals

The JAXA-ESA-NASA LANS interoperability demonstration mission aims to validate the end-to-end performance of the initial instantiation of LANS comprised by one ESA Moonlight LCNS node, one Japanese LNSS node and at least two NASA LCRNS nodes. The demonstration lander is expected to host at least two LANS receivers to acquire, track and process the AFS broadcast by the different nodes contributing to the LANS. Hence, providing a direct means to verify the interoperability between the different LNSPs. "Truth" data will be generated using independent measurements and processing to enable the verification.

Concretely, the following objectives are defined for the demonstration:

- OBJ-1. To receive AFS from each LNSP node and assess the signal quality
- OBJ-2. To compute and validate the SISE for each LNSP node
  - I. To estimate the LNSP node orbit SISE contribution
  - II. To estimate the LNSP node clock SISE contribution
  - III. To evaluate contributing error sources (e.g., the LNSP node hardware delay)
- OBJ-3. To validate the achieved user Position, Velocity, and Time (PVT) knowledge from combined LANS
  - I. To estimate the User Equivalent Ranging/Range Rate Error (UERE/UERRE) per LNSP node
  - II. To estimate the different user Dilution of Precision (DOP) metrics
- OBJ-4. To validate the LunaNet time and Reference Frame

Given that more than one LANS receiver will be available on the demonstration lander, raw data can be exchanged between the agencies involved to have additional sources for validation (i.e., checking consistency).

2.1 [OBJ-1] AFS reception and quality assessment

The demonstration lander receipt of the AFS signals on the lunar surface will provide a unique opportunity for in-situ reception and quality assessment of the AFS as broadcast from multiple LNSPs. The elements that can be validated by reception of AFS at the lander are:

- AFS received carrier-to-noise density ratio (C/N0) compared to the expected C/N0 based on power-on-surface link budget analyses;
- AFS navigation message received compared to the products available from providers;
- AFS signal quality (e.g., signal coherency, correlation loss, etc.).

The expected C/N0 can be evaluated based on the known satellite Effective Isotropic Radiation Power (EIRP) for the given LNSP node, the satellite antenna gain, the free-space path loss calculated between the known satellite and receiver positions, as well as the receiver gain and noise contribution.

2.2 [OBJ-2] LNSP SISE computation and validation

The SISE is one of the key system drivers for the performance of the AFS. It captures the system contribution to the range and range-rate error between the AFS transmitting node and any user, and heavily influences the user PVT solution accuracy.

2.2.1 SISE Position

Eq. (1) shows the LunaNet definition of SISE position [2], where x, y, z, t are the true 3-axis position and time, while the corresponding tilde parameters represent the values broadcast in the navigation message.

$$SISE_{pos} = \sqrt{(x-\tilde{x})^2 + (y-\tilde{y})^2 + (z-\tilde{z})^2 + (ct-c\tilde{t})^2} \tag{1}$$

The $SISE_{pos}$ is the combination of estimation and prediction errors for both the LNSP node orbit and clock. The ranging error effecting the receiver measurements is impacted by the SISE, considering the projection of the SISE to the LNSP to user line-of-sight, and the user equipment error (UEE). This ranging error is referred to as the User Equivalent Ranging Error (UERE) as shown in Eq. (2), where $\overrightarrow{\mathrm{SISE}}_{pos,orbit}$ represents the first three terms of Eq. (1) in vector format, $\vec{e}_{rx}^{sat}$ is the unit vector from the LNSP node to the lander. Note that for the UERE $\overrightarrow{\mathrm{SISE}}_{pos,orbit}$ is projected on to the satellite-receiver line-of-sight vector. $SISE_{pos,clk}$ captures the error in clock knowledge and any uncalibrated hardware delays in the LNSP node transmission, as represented by the last term of Eq. (1).

$$UERE = \sqrt{UEE^2 + \left(\overrightarrow{SISE}_{pos,orbit} \cdot \vec{e}_{rx}^{sat}\right)^2 + SISE_{pos,clk}^2} \tag{2}$$

In the lunar environment, the UEE is driven by:

- Receiver thermal noise (assumed Gaussian) linked to the configuration of the Delay Locked Loop (DLL)
- Multipath
- LANS receiver instrument delays

The Moon does not have an atmosphere, and its very thin exosphere does not significantly impact the UEE. However, the multipath environment characterization for S-band navigation signals on the Moon needs to be improved. Therefore, measurements at low elevation shall be avoided for SISE validation purposes to limit the impact of multipath on this demonstration.

To validate the UERE, the following additional information is required, beyond that received via AFS:

- Precise location of the lander, which will be surveyed using laser ranging and DTE as discussed in Section 2.3;
- Estimation of the receiver clock (see Section 2.3);
- Precise a-posteriori orbits of the LNSP nodes generated by the providers (e.g., similar to GNSS precise products); and
- Precise a-posteriori clock products of the LNSP nodes generated by the providers (e.g., similar to GNSS precise products).

The pseudorange measured by the receiver is indicated in Eq. (3), where $\vec{x}_{sat}$, $\vec{x}_{rx}$, t_{rx}, $\mathrm{K}_{P,Rx}$, $\mathcal{M}_P$, Δt_{rel}, and ϵ_P reflect, respectively, the LNSP node position, the lander position, the lander clock bias, LANS receiver instrument

delays, multipath, relativistic delays, and the error induced by the receiver thermal noise. Note that the instrument delays refer to delays that are not calibrated.

$$\rho = |\vec{x}_{sat} - \vec{x}_{rx}| + c\left(dt_{rx} + \mathrm{K}_{P,Rx} + \Delta t_{rel}\right) + \overrightarrow{SISE}_{pos,orbit} \cdot \vec{e}_{rx}^{sat} + SISE_{pos,clk} + \mathcal{M}_P + \epsilon_P \tag{3}$$

As the LNSP node position, clock, and receiver clock bias are known (see Section 2.3), assessing the difference between the measured pseudorange and the geometric one-way slant range as calculated from the "truth" data yields the UERE that contains the following elements:

- SISE orbit position, as a projection onto the satellite-to-lander line-of-sight
- SISE clock (accounting also for uncalibrated instrument errors at satellite level)
- Uncalibrated instrument errors at lander level
- Multipath error contribution
- Estimation errors in the precise a-posteriori products
- Unmodelled relativistic delays

This collection of information can then be used to characterize the SISE position of the LNSP nodes.

2.2.2 SISE Velocity

The SISE velocity is shown in Eq. (4) where the dotted variables represent the true velocity in x, y, z components, respectively, and ṫ represents the LNSP node clock drift. The corresponding tilde parameters represent the values broadcast in the navigation message.

$$SISE_{vel} = \sqrt{\left(\dot{x} - \tilde{\dot{x}}\right)^2 + \left(\dot{y} - \tilde{\dot{y}}\right)^2 + \left(\dot{z} - \tilde{\dot{z}}\right)^2 + \left(c\dot{t} - c\tilde{\dot{t}}\right)^2} \tag{4}$$

Similarly to the $SISE_{pos}$, the $SISE_{vel}$ is a combination of estimation and prediction errors of both the LNSP node orbit and clock. The User Equivalent Range-Rate Error (UERRE) is defined in Eq. (5). In this equation $\frac{d}{dt}(UEE)$, $\overrightarrow{SISE}_{vel,orbit}$, and $SISE_{vel,clk}$, respectively, indicate the derivative of the UEE, the SISE orbit contribution linked to the first three terms of Eq. (4), the SISE clock error contribution and the derivative of the hardware biases captured by the last term of Eq. (4).

$$UERRE = \sqrt{\frac{d}{dt}(UEE)^2 + \left(\overrightarrow{SISE}_{vel,orbit} \cdot \vec{e}_{rx}^{sat}\right)^2 + SISE_{vel,clk}^2} \tag{5}$$

In the lunar environment, the derivative of the UEE is driven by:

- Receiver thermal noise (Gaussian) linked to the configuration of the Frequency Locked Loop (FLL) or the Phase Locked Loop (PLL)
- LANS receiver uncalibrated frequency oscillator offsets
- LANS receiver uncalibrated phase differences (i.e., offset and variation)

Similar to the SISE position validation, additional information is required for validating SISE velocity, beyond what is received via AFS. It is assumed that the external information required for the SISE position (as shown in Section 2.2.1) also includes the velocity-related components, such as the LNSP node velocity, clock drift, and receiver clock drift. The range-rate, $\dot{\rho}$, can subsequently be modelled as shown in Eq. (6). The dotted quantities represent the derivative of the parameters shown in Eq. (3) with the SISE position contributions replaced by those for SISE velocity.

$$\dot{\rho} = \frac{\left(\vec{\dot{x}}_{sat} - \vec{\dot{x}}_{rx}\right) \cdot \left(\vec{x}_{sat} - \vec{x}_{rx}\right)}{|\vec{x}_{sat} - \vec{x}_{rs}|} + cd\dot{t}_{rx} + \overrightarrow{SISE}_{vel,orbit} \cdot \vec{e}_{rx}^{sat} + SISE_{vel,clk} + \dot{\mathrm{K}}_{P,Rx} + \dot{\epsilon}_P \tag{6}$$

Given that the LNSP node velocity, clock drift, and receiver clock drift are known (see Section 2.3), assessing the difference between the measured pseudorange-rate and the geometric range-rate as calculated from the "truth" data yields the UERRE that contains the following elements:

- SISE orbit velocity, as a projection onto the satellite-to-lander line-of-sight
- SISE clock drift
- Uncalibrated frequency offsets in the lander and satellite instruments

- Estimation errors in the precise a-posteriori products

The UERRE can then be used to characterize the SISE velocity of the LNSP nodes.

2.3 [OBJ-3] Combined LANS user PVT validation

The LANS receivers within the lander will compute a PVT solution which needs to be validated with a "truth" PVT. The "truth" position and velocity are generated on the ground based on the following measurements:

- Satellite Laser Ranging (SLR) two-way range measurements between the lander and Earth-based laser ranging stations;
- Two-way range, carrier phase, and Doppler measurements between the lander's Tracking, Telemetry, and Command (TT&C) transponder and Earth TT&C station (i.e., DTE radiometric ranging);
- Delta-Differenced One-Way Ranging (DDOR) measurements of the lander and a subset of LNSP nodes.

Note that the lander's velocity estimate is expected to be zero since the lander is stationary.

The receiver clock "truth" can be estimated using one of the following time-transfer techniques. A baseline approach will be consolidated in the future.

- Two-way satellite time-transfer using the TT&C link either synchronously or asynchronously;
- Terrestrial Global Navigation Satellite System (GNSS) based time-transfer (one-way);
- AFS based time-transfer assuming a known lander position.

Once the lander's "truth" PVT is available, it can be compared to the interoperable LANS-derived PVT solution to quantify the accuracy and precision of the LANS-derived PVT solution.

2.4 [OBJ-4] Validation of LunaNet Time and Reference Frame

There are multiple areas that can be validated concerning lunar time and reference frames during the LANS demonstration. First, the interoperability of the Clock and Ephemeris Data (CED) of the different LNSP nodes can be assessed. Following the LunaNet Applicable Document 5 (AD-5) on interoperable aspects of time and reference frames, each LNSP node should refer to a common time (i.e., LunaNet Reference Time (LRT)) and provide the ephemeris in a common reference frame (e.g., lunar Principal Axis (PA) frame). For practical reasons, each LNSP may have its own time realization (i.e., LNSP System Time (LST)) and will provide the user with a prediction of the LST-LRT offset. This accuracy with which this offset is predicted by each LNSP, however, is not perfect and may introduce errors to the UERE. Similarly, LNSPs may not use the same realization of the reference frame requiring the LNSP to provide the user with the transformation to the common reference frame realization, which may introduce errors.

The measurements from AFS made by the LANS receivers will be sent to the ground for offline processing. Employing the LNSP precise products used for SISE validation, it is possible to characterize the actual offset between LST and LRT and thus assess the impact of the LST-LRT prediction upon the user PVT solution. Moreover, a-posteriori navigation products for each LNSP can be reprocessed using one identified frame realization, thereby allowing an assessment of the impact on user PVT from using different frame realizations.

An atomic clock located on the lunar surface (an option currently under consideration) with the capability to trace its output to a terrestrial timescale by means of two-way time-transfer (see Section 2.3) may enable the characterization of relativistic variations. The ability to resolve these relativistic differences depends on the clock stability. The ability to measure these relativistic variations could enable estimating the linear and the dominant periodic terms that characterize the relation between UTC and the proper time of a clock resting on the Moon surface. Furthermore, this data could be assessed as part of a bigger picture comparing the atomic clock behavior (driven by relativistic effects which vary along the LNSP node orbits due to their eccentricity) within the demonstration lander to the atomic clock behavior measured by the LNSP nodes, depending on the LNSP node clock steering strategy.

Finally, a laser retroreflector on the lunar surface (equipped on the demonstration lander) within the vicinity of the South Pole could enable improvement of the realizations of the PA frame (or lunar reference frames in general) by adding additional points that can be surveyed with Lunar Laser Ranging (LLR) stations on Earth.

3. Demonstration Architecture

Figure 2 depicts the architecture plan for the LANS interoperability demonstration mission. The JAXA-ESA-NASA LANS interoperability demonstration mission, currently targeted for 2029, aims to contribute to verifying interoperability of the available LANS that is expected to be composed of AFS broadcast from a Japan LNSS satellite, an ESA LCNS satellite, and three NASA LCRNS satellites. Placing the LANS receiver(s) in the lunar SP region allows them to capture the AFS broadcast by these LNSP nodes, and verify interoperability among these lunar PNT systems in an overlapping service area. Although still under investigation, the lander is expected to include one laser

retroreflector (LRR) and one miniature Rubidium Atomic Frequency Standard (MiniRAFS) to enable the determination of the lander "true" position and clock reference. By using these assets, the achieved SISE associated with each LNSP satellite, along with the joint LANS PVT performance, will be evaluated by exchanging relevant data between the three space agencies (ESA, JAXA, and NASA) (see section 2.2).

Figure 3 illustrates the asset deployment plan for the LANS interoperability demonstration mission. Per the current plan, JAXA's H3 rocket will launch a lander with two demonstration components: the Japan LNSS demonstration satellite and LANS interoperability demonstration payload, including receivers. This lander will deploy this LNSS satellite into a lunar polar orbit and then land on the lunar South Pole (SP) region with the hosted payload.

The threshold objective for this demonstration mission is to show that at least two AFS, each from a different LNSP, can be received and processed by each LANS receiver simultaneously. A goal for reception of four simultaneous AFS allows a joint LANS PVT accuracy evaluation by comparing each LANS receiver's PVT solution with the "truth" solution. The mission data acquisition and concept for the evaluation of the "truth" data are illustrated in Fig. 4. The mission data refer to the in-situ real-time data consisting of the received AFS raw measurements and the LANS receivers' PVT solutions. Furthermore, LNSP node mission data includes observations, clock, and ephemeris solutions from each node. For example, LNSS node mission data includes observations from GNSS weak signals received by the LNSS satellite. As applicable, these mission data will be transmitted to Earth ground stations via the data transmission link of the LNSP node, the lander's transmitter, or using other available lunar relay nodes such as the ESA's Lunar Pathfinder.

The "truth" data are composed of the LNSP node precise orbit and onboard clock data (similar to GNSS precise products) and the LANS receiver's precise position and clock data. The "truth" data will be used to validate the LANS receiver interoperable PVT and the SISE of the LNSP nodes as identified in Section 2. The LNSS satellite precise orbit will be determined by using traditional X-band DTE ranging and Delta-Differential One-way Ranging (DDOR), while the LCNS satellite precise orbit will be determined using X-band DTE ranging and lunar laser ranging. Then, based on these precise orbit determination results, the satellite clock data will be estimated by using the downlinked observations from GNSS weak signals received by the LNSS, while for the LCNS satellite, the clock offset will be estimated by two-way satellite time-transfer. Methods for obtaining independent reference orbit and clock determination approaches for the demonstration for the LCRNS satellites are under investigation. The precise LANS receiver's position will be determined based on terrestrial based ranging (i.e., DTE ranging and lunar laser ranging (LRR)). Then, based on these precise position results, the receiver's clock will be estimated. This concept is identified in Section 2.

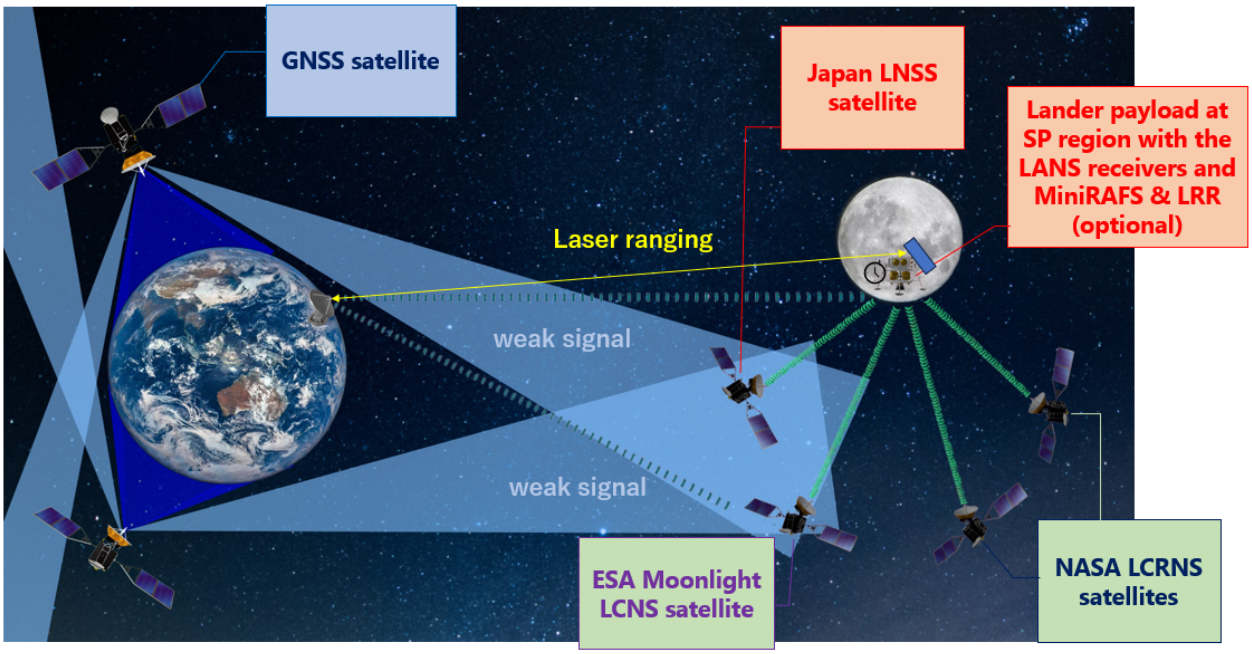

Fig. 2 LANS interoperability demonstration architecture plan.

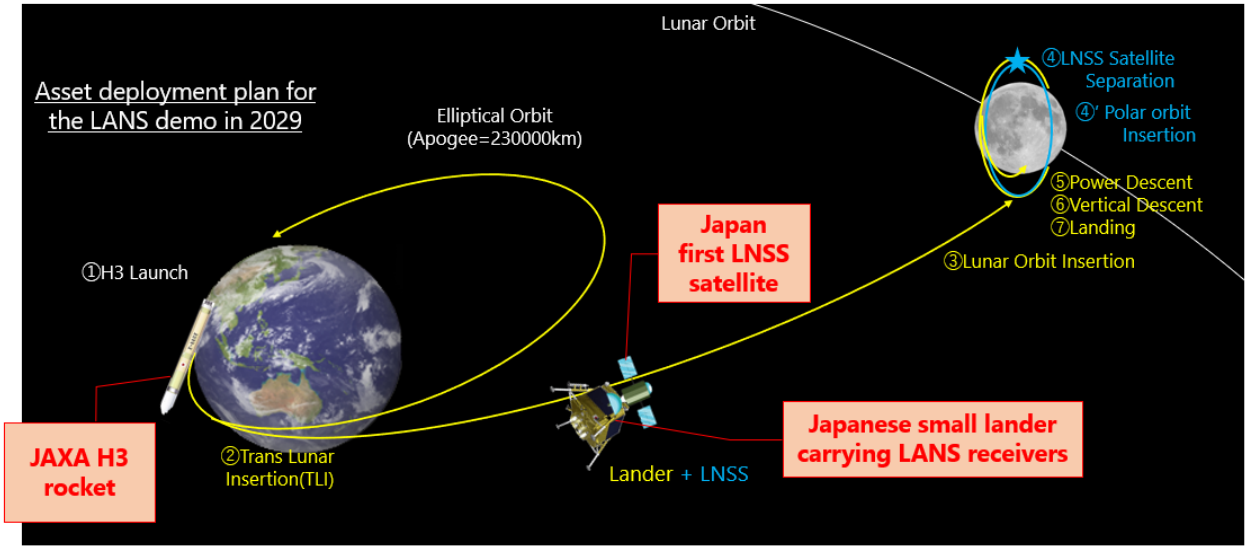

Fig. 3 Asset deployment plan for the LANS demonstration mission targeted for 2029.

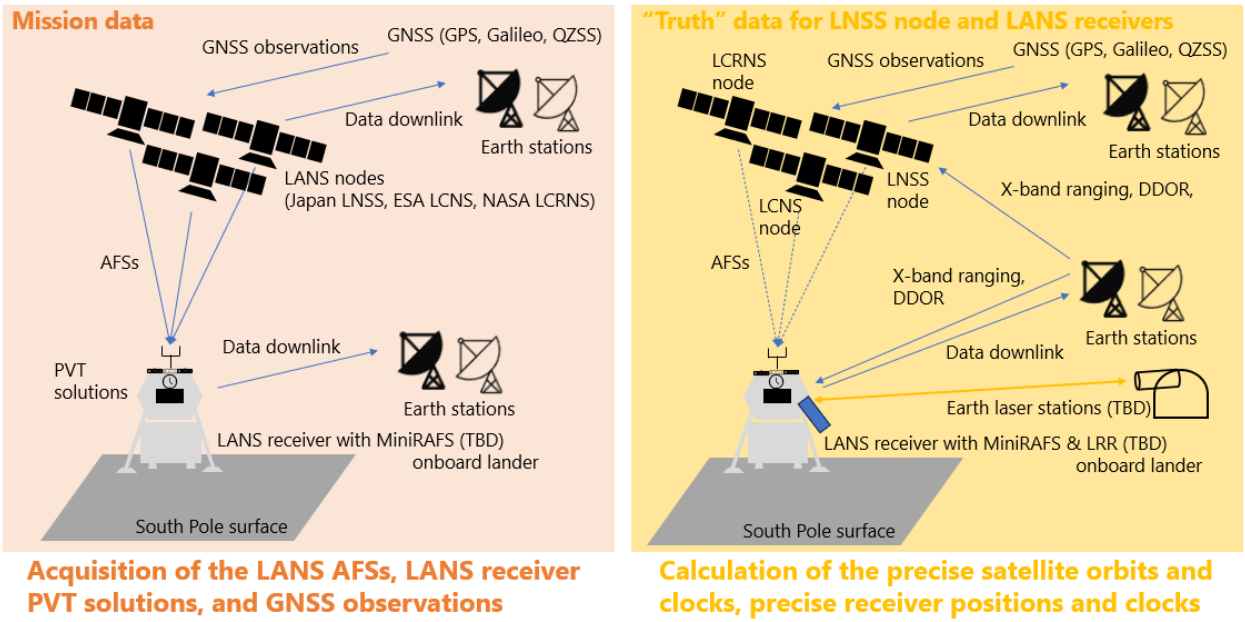

Fig. 4 Mission data acquisition and "truth" data calculation.

4. Demonstration Mission Assumptions

The assumptions for this demonstration mission are as follows:

- ESA and NASA orbital assets are in place prior to launch of the demonstration payload,
- LNSS demonstration satellite will be delivered and deployed by a Japanese small lander carrying the demonstration payload,
- LNSS demo satellite will be commissioned prior to executing the LANS interoperability demonstration,
- Antenna and LNA will provide appropriate gain to noise temperature ratio to the LANS receivers,
- Pre-flight integration will characterize the performance of each LANS receiver,
- All LANS receivers will have the capability to use the same clock as the reference source,
- Data will be shared among the space agencies (JAXA, ESA, NASA), including the capture of raw measurements from each LANS receiver,
- Data reduction will mitigate multi-path impacts, e.g. by applying elevation angle constraints,

・Availability of Satellite Laser Ranging (SLR) stations as needed during the demonstration period,

・Availability of and adequate line of sight to two deep space ground stations for DDOR as needed during the demonstration period,

・Lander lifetime and power are sufficient to achieve all the mission objectives.

The LANS initial service will be available in the lunar SP region within a latitude less than -80 degrees. For this LANS interoperability demonstration mission, the LANS receivers will be landed at a location within the defined service region that is visible to Earth and SLR ground stations for the sake of direct-to-earth mission data transmission and offline "truth" data calculation using data from these stations. Each LANS receiver will calculate its PVT solution in real-time based by processing measurements extracted from the received AFS. To reduce the vertical positioning errors, height (elevation) values computed from digital elevation maps (DEM) will be incorporated into these receiver's filtered PVT solutions [11][12].

5. Payload Overview

Figure 5 illustrates the interoperability demonstration payload to be delivered by a lander. The LANS receivers from Japan, ESA, and NASA (TBD) will be all connected to the same antenna and clock; here, we assume the use of a miniature Rubidium Atomic Frequency Standard (MiniRAFS) as the clock reference. The laser retroreflector (LRR) may be onboard the lander for precise position determination purposes. The DTE link is for the mission data transmission to Earth operation stations.

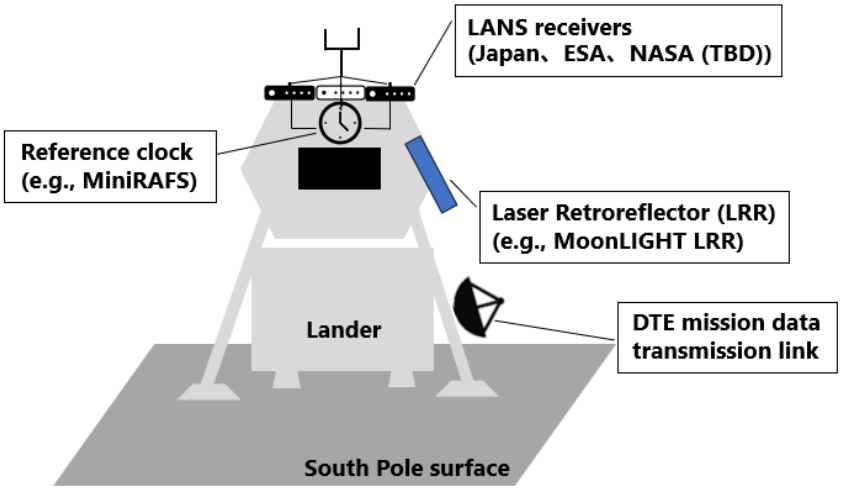

Fig. 5 Illustration of the lander payload.

6. Concept of Operations

The three space agencies, JAXA, ESA, and NASA, are now developing the Concept of Operations (ConOps) for this LANS interoperability demonstration mission. As shown in Fig. 6, the demonstration operation begins by with step 1 to collect the mission data, of which there are two portions. The first collection is to establish "truth" PVT solutions for all LNSP nodes transmitting the AFS and for the LANS demonstration payload. The second collection includes AFS observables and LANS PVT solutions generated by the LANS receivers. In step 2 of the demonstration, "truth" data is calculated/estimated offline using the mission data from step 1. Step 3 performs a comparison of AFS SISE and experiment PVT solutions against the "truth". For the in-depth analysis of the SISE, the comparison between the received pseudorange measurements with the calculated "truth" pseudorange values becomes essential to identify unknown ranging error sources such as satellite hardware delays and delays associated with the Moon's environment. Data sharing among the three space agencies is paramount to the success of this mission.

Three major steps for the demonstration

1. Acquisition of mission data (observations from the AFSs and terrestrial GNSS, LANS receiver PVT solutions) in Moon's environment
2. Calculation of "truth" data (precise LANS satellite orbits and clocks, precise LANS receiver positions and clocks) by Earth stations and laser stations (TBD)
3. Evaluation of SISEs for LNSP nodes and LANS PVT accuracy by comparing the acquired mission data with the calculated "truth" data

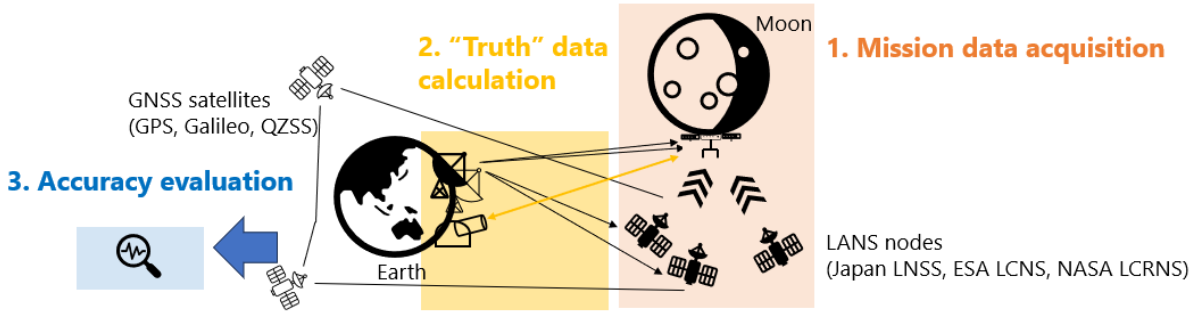

Fig. 6 Three major steps for the LANS interoperability demonstration.

7. Preliminary Analysis

To understand the attainable positioning performance of the lander payload for the LANS interoperability demonstration, a high-level analysis has been performed. The approach is based on the methodology presented in earlier publications [11][12] that assessed the performance of a lunar rover using Moonlight LCNS.

7.1 LANS Assumptions

For this analysis the instantiation of LANS is considered with one ESA Moonlight LCNS node, one Japanese LNSS node and three NASA LCRNS nodes per its IOC-B increment. High level design parameters of the LNSP node orbits are provided in Table 1. It should be noted that the orbits and EIRP are notional and are only applicable for a preliminary performance analysis within the context of the LANS interoperability demonstration.

Table 1. LNSP Node Orbits (in EOP frame), note that all parameters are notional. The confidence interval for the SISE is different per LNSP to represent the performances specified by the different systems.

	ESA Moonlight LCNS NAV #1	Japan LNSS Demo	NASA LCRNS #1	NASA LCRNS #2	NASA LCRNS #3
Orbital Period	24 hrs	6 hrs	32.8 hrs	32.8 hrs	32.8 hrs
Eccentricity	0.7	0	0.678	0.678	0.678
EIRP at boresight	25 dBW	14 dBW	26.7 dBW	26.7 dBW	26.7 dBW
SISE-pos	20 m (2-sigma)	20 m (2-sigma)	13.43 m (3-sigma)	13.43 m (3-sigma)	13.43 m (3-sigma)

The LNSP node antenna patterns selected for this analysis ensure the field-of-view (i.e., half-power beamwidth) covers at least the full footprint of the Moon. Furthermore, the EIRP selected complies with the power-on-surface requirements as specified in the LSIS AD1 [2]. This means that for each LNSP, visibility is defined when the satellite is in the user line-of-sight (i.e., when the satellite is not occulted by the Moon and the elevation from the lander to the LNSP node is above 0 degrees).

The SISE is modelled based on the value reported in Table 1, where the model depends on the LNSP node:

- For Moonlight LCNS, the SISE was modelled considering the age-of-data (AOD) effect based on the approach detailed in [12].
- For the Japan LNSS and the NASA LCNRS, the SISE is modelled as shown in Eq. (7) and (8).

$$\Delta\vec{x} = \begin{pmatrix} \mathcal{N}\left(\mathcal{N}\left(0, SISE_{pos,orbit}\right), 0.1 \cdot SISE_{pos,orbit}\right) \\ \mathcal{N}\left(\mathcal{N}\left(0, SISE_{pos,orbit}\right), 0.1 \cdot SISE_{pos,orbit}\right) \\ \mathcal{N}\left(\mathcal{N}\left(0, SISE_{pos,orbit}\right), 0.1 \cdot SISE_{pos,orbit}\right) \end{pmatrix} \quad (7)$$

$$\Delta t = \mathcal{N}(SISE_{pos,clk}, 0.1 \cdot SISE_{pos,clk}) \quad (8)$$

Where $\mathcal{N}(\mu, \sigma^2)$ represents a Gaussian distributed variable with a mean μ and a standard deviation σ. In this case the following relation is applicable: $SISE_{pos} = \sqrt{SISE_{pos,orbit}^2 + SISE_{pos,clk}^2}$, where for the NASA and Japanese LNSP nodes, $SISE_{pos,clk}$ is set to 1 meter. This is a high-level assumption that is not considered representative of the actual system performance.

7.2 *User Assumptions*

The demonstration lander is assumed to be equipped with a hemispherical patch antenna [11] with a boresight antenna gain of 6 dBi (as shown in Fig. 7), and a LANS receiver that is representative of a space-based GNSS receiver with a receiver noise temperature of 113 K [13], a state-of-the-art low noise amplifier (LNA), a DLL, and a PLL to track the AFS Pseudorandom Noise code and radio frequency carrier. The configuration of the LNA and tracking loops are provided in Table 2.

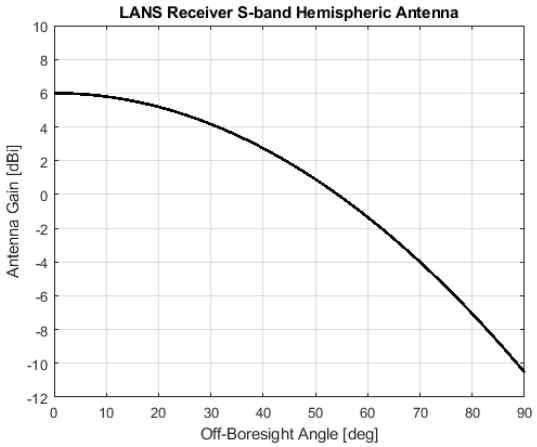

Fig. 7. LANS Receiver antenna pattern.

Table 2. Characteristics of the LANS receiver.

Parameter	Value	Unit
RF Front-End (RFFE) Characteristics		
RFFE Noise Figure	1	dB
Antenna Noise Temperature [13]	113	K
LNA Gain	30	dB
Tracking Loop Characteristics		
DLL Bandwidth	0.5	Hz
FLL Bandwidth	10	Hz
Coherent Integration Time	20	ms
Early-late Spacing	1	Pilot Chip

For the purposes of this study, the following assumptions were made to provide an estimate of performance.

- The lander is located at a latitude of -87 degrees and a longitude of 20 degrees East.
- The LANS receivers are assumed to use an OCXO (oven-controlled crystal oscillator). The Allan Deviation of the OCXO is provided in Table 3 [11]. Additionally, the performance with a MiniRAFS was assessed as well. Therefore, its Allan Deviation is also included in Table 3.

Table 3. OCXO and MiniRAFS LANS receiver clock specification.

Allan Deviation	OCXO	MiniRAFS
τ = 1 s	1e-10	1e-11
τ = 10 s	3e-10	3e-12
τ = 100 s	3e-10	1e-12
τ = 1,000 s	2e-10	3e-13
τ = 10,000	n/a	1e-13
τ = 86,400 s	1e-12	n/a

Note that the actual demonstration intends to include a MiniRAFS clock, which will improve the achievable performance.

7.3 *Simulation Framework*

The PVT for the lander is estimated using an EKF with a height constraint (that is provided through a digital elevation model (DEM)). The architecture of the EKF and the DEM approach are further detailed in [11] and [12], respectively. The DEM is considered as an additional observable from the lander to the center of the Moon without a clock contribution. As shown in Eq. 9, the difference between a normal LANS measurements at the top and the DEM measurement at the bottom can be observed. The uncertainty of the DEM measurement is a function of the accuracy of the DEM and the position covariance of the filter as further detailed in [11].

$$H_\rho = \begin{bmatrix} -\frac{\boldsymbol{x}_u^{1\,T}}{|\boldsymbol{x}_u^1|} & \mathbf{0}_{1\times3} & 1 & 0 \\ \vdots & \vdots & \vdots & \vdots \\ -\frac{\boldsymbol{x}_u^{DEM\,T}}{|\boldsymbol{x}_u^{DEM}|} & \mathbf{0}_{1\times3} & 0 & 0 \end{bmatrix} \tag{9}$$

For the purposes of this analysis, it is assumed that all LNSP nodes are synchronized to the same reference clock and disseminate their navigation products in the same reference frame. This is a simplification as in reality likely each system may have its own system timescale as further described in Section 2.4.

The range and range-rate measurements are simulated as per Eq. 10 and Eq. 11.

$$\rho = |r_s - r_u| + \Delta t_u + \Delta t_{sv} + \epsilon_{DLL} \tag{10}$$

$$\dot{\rho} = \frac{\left(\vec{r}_s - \vec{r}_u\right) \cdot (\vec{r}_s - \vec{r}_u)}{|\vec{r}_s - \vec{r}_u|} + \Delta \dot{t}_u + \Delta \dot{t}_{sv} + \epsilon_{FLL} \tag{11}$$

In Eq. 10, $\underline{r_s}$ and $\underline{r_u}$ refer to the satellite and user position, respectively. Similarly, the dotted variables in Eq. 11 represent the satellite and user velocity. In these equations, Δt_{sv} and $\Delta \dot{t}_{sv}$ represent the satellite clock error bias and drift that cannot be corrected by the navigation message; Δt_u and $\Delta \dot{t}_u$ represent the user clock bias and drift contribution; $\underline{\epsilon_{DLL}}$ and $\underline{\epsilon_{FLL}}$ represent the error contribution to the thermal noise of the receiver, considering the code is tracked by a Delay Locked Loop (DLL) and the Doppler frequency by a Frequency Locked Loop (FLL). Note that $\underline{\epsilon_{DLL}}$ and $\underline{\epsilon_{FLL}}$ are a function of the tracked C/N_0 as well as the tracking loop parameters introduced in Table 2 based on well-known GNSS models [14].

7.4. *Simulation Results*

Within this study, both pseudorange and Doppler measurements are processed, and results without and with a height constraint based on application of DEM, are provided respectively in Section 7.4.1. and 7.4.2. Note that the results in this paper represent only a single run. It should be remarked that in both cases, with and without height constraint, the user clock is estimated by the receiver, e.g. 4 dimensional (4D), but the receiver estimated clock bias is not reported.

7.4.1. Without height constraint

Fig. 8 shows the visibility of LNSP nodes for the period of one Earth day. As noted above, the orbits are notional and subject to change. Throughout this day, at least 3 satellites are visible all the time. The Japanese LNSS satellite with its 6-hour orbital period has a roughly 2-hour visibility window every 6 hours, thus occur between 2 and 4, 8 and 10, 14 and 16, and 20 and 22 hours of the simulation. The first window overlaps with one of the LCNS or LCRNS satellites disappearing behind the lunar lander horizon resulting in a short period with 5 satellites in view. Due to the eccentric orbits (especially the LCRNS 32-hour orbits), a minimum of 3 satellites are visible above the South Pole. This varies from day to day. Fig. 9 shows the Dilution Of Precision (DOP) for the window between 8 and 24 hours. The DOP captures the impact of the constellation geometry into the user PVT error (i.e., $\underline{\sigma_{PVT} = UERE \times DOP}$). Different formulations of DOP exist, where GDOP represents the geometric DOP (4D), PDOP the positioning DOP (3D), and HDOP the horizontal DOP (2D) [16]. For GNSS systems, a Geometric DOP (GDOP) < 5 is generally

considered "good". In the classical definition, the DOP is only defined when at least 4 satellites are visible that are required to estimate the 3D position and receiver clock error. Therefore, in Fig. 9, the DOP is only defined when four satellites are in view. Furthermore, the DOP shows a large variation reaching values up to 10^4. It should be noted that the relative phasing of the LNSP orbits is not optimized and that the DOP can be improved by proper phasing of the LNSP nodes.

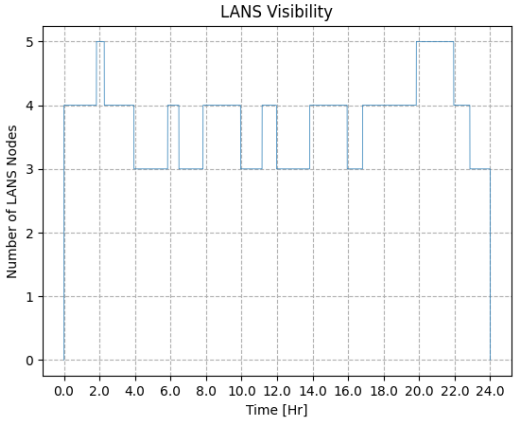

Fig. 8. LNSP node visibility of the LANS receiver.

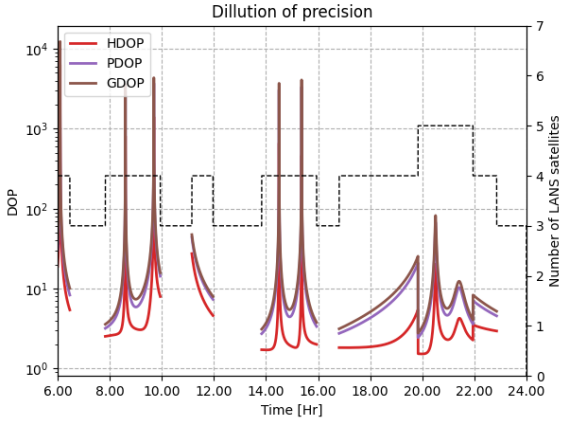

Fig. 9. Dilution of precision (2D, 3D, 4D).

Fig. 10 and Fig. 11 provide the position error (compared to the "true" trajectory) for the horizontal (2D) and 3D position, respectively. The yellow shaded area indicates the covariance provided by the Extended Kalman Filter (EKF). Note that in some cases, the covariance of the filter substantially over bounds the actual positioning error. This can be further improved by tuning the EKF, which is part of future studies. Comparing these figures to Fig. 8 clearly shows the link between positioning accuracy and DOP, where the 2D position error reaches values near 100 meters during periods when the DOP "peaks". Between hours 17 and 20, when the DOP is < 10, a 2D positioning error around or better than 10 meters is observed. Between 17 and 20 hours, the 3D position error achieves a 10m level with is in line with the positioning requirements set by Artemis [15].

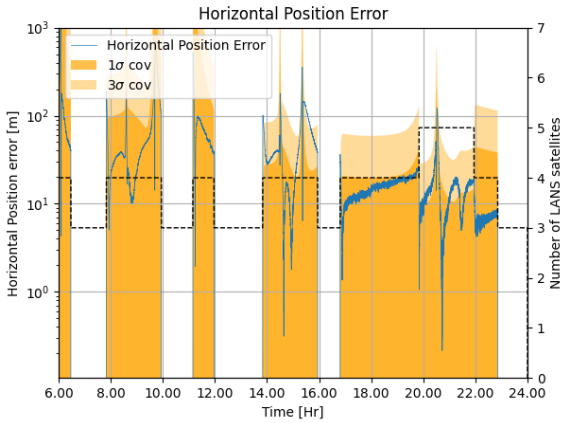

Fig. 10. Horizontal (2D) position error for the LANS receiver without a height constraint, based on an OCXO.

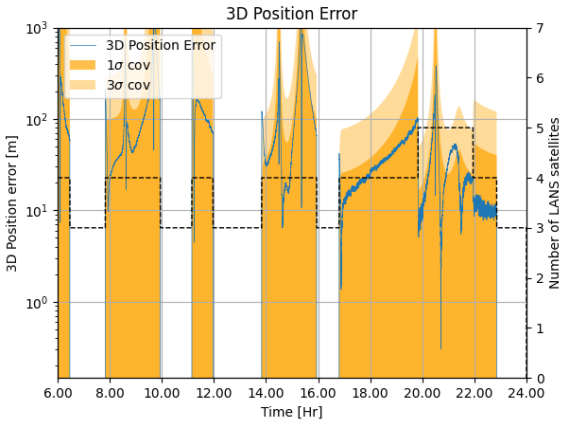

Fig 11. 3D position error for the LANS receiver without a height constraint, based on an OCXO.

Table 4 provides the position error statistics without a height constraint, when at least four satellites are visible. Even though there are a substantial period in which the position error is large due to the high DOP (i.e., a GDOP well above 5), the mean error is only 13.5 meter (both horizontal (2D) and 3D). The higher percentiles, however, attain larger error values, as expected due to the high DOP. Furthermore, the 3D positioning error is larger for the higher percentiles. This is related to the fact that, similar to GNSS, the height of the receiver is correlated to the user receiver clock and therefore more difficult to observe.

Table 4. Position error statistics without height constraint.

	Mean Error [m]	Error (68-perc) [m]	Error (95-perc) [m]	Error (99.7-perc) [m]
2D (OCXO)	35.7	25.0	121.6	362.0
3D (OCXO)	87.6	60.5	346.1	935.5
3D (MiniRAFS)	36.3	26.8	136.4	310.0

7.4.2. With height constraint

Fig. 12 shows the dilution of precision of the LANS receiver with a height constraint (refer to section 7.3). Comparing this to Fig. 9 it should be noted that the magnitude of the DOP is much lower (i.e., each DOP < 5 for the full duration). Furthermore, the DOP is always available even when 3 satellites are visible by the LANS receiver due to the height constraint compensating for the vertical, *z*, dimension.

Fig. 13 gives the horizontal (2D) position error for the height constrained positioning filter. Compared to Fig. 11, the error is substantially reduced due to the absence of the extreme DOP "peaks". Throughout the full window, the 2D error is close to or below 10 meters.

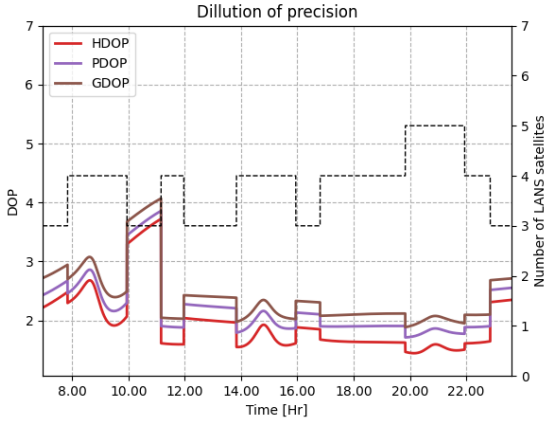

Fig. 12 Dilution of Precision (2D, 3D, and 4D) with a height constraint.

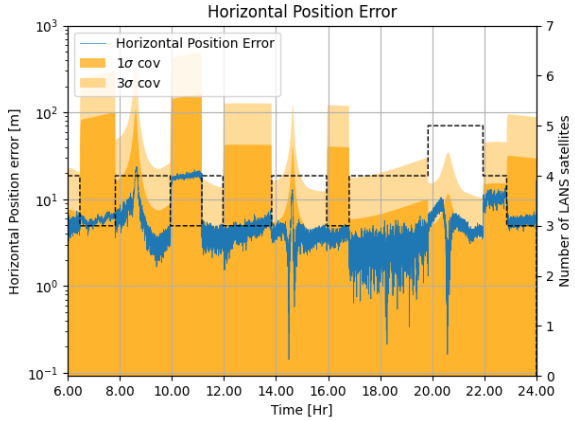

Fig. 13. Horizontal (2D) position error and covariance for the lander with a height constraint, based on an OCXO.

Finally, Table 5 provides the statistics of the position error of the LANS receiver with height constraint. The error is much lower than the case without height constraint and only the 99.7 percentile exceeds 10 meters. Furthermore, the difference between the 2D and 3D position error is small. This is related to the fact that the vertical position is constrained by the DEM. As a result, the 3D error is mostly driven by the horizontal (2D) position accuracy.

Table 5. Position error statistics with height constraint.

	Mean Error [m]	Error (68-perc) [m]	Error (95-perc) [m]	Error (99.7-perc) [m]
2D (OCXO)	5.7	5.6	17.2	19.5
3D (OCXO)	6.5	6.4	17.6	19.9
3D (MiniRAFS)	5.4	5.9	8.2	8.9

To show the impact of the receiver clock on the position estimate, another simulation was performed with a MiniRAFS clock, compared to the OCXO that was baselined. Comparing the 3D solutions using the OCXO and the MiniRAFS shows that with the more stable clock (e.g. MiniRAFS) the position result also improves. Such an approach is considered reasonable as the demonstration lander will potentially equipped with a MiniRAFS which has low SWaP.

8. Future Endeavors

While the LANS Interoperability demonstration intends to take place with NASA's LCRNS IOC-Bravo capabilities, the next increment, IOC-Charlie, will increase the South Pole service volume to -75 degrees and 200 km

altitude, and increase the number of LNSP nodes simultaneously in view to four, meeting a GDOP<6 over 40% of an Earth day. As the user community needs for additional capability grow, NASA can evolve the lunar PNT service offerings appropriately, in accordance with M2M Objective LI-3, to develop a lunar position, navigation, and timing architecture capable of scaling to support long term science, exploration, and industry needs.

During the LANS interoperability demonstration, Moonlight LCNS will be in its IOC phase. The constellation will be further complemented by 3 additional navigation satellites in 2030 which declare Moonlight FOC. During FOC, the service is targeting a Height-constrained Horizontal Dilution of Precision (HHDOP)—the HDOP calculated assuming height information is provided by external sensors or data (e.g., digital elevation models)—of less than 3.5 for at least 15 hours per Earth day across the Moon's South Pole region (-70 to -90 degrees latitude). Furthermore, the SISE will be improved from 20 meters (at IOC) to 10 meters for at least 95% of the time. This Moonlight architecture aims to provide lunar users with positioning accuracies of 10 meters for surface rovers, 50 meters for landers, and 100 meters for orbiters. The Moonlight service has been conceived to be expandable, which means additional satellites could be added in the future to enhance the Moonlight service availability or increase the lunar coverage area.

Furthermore, as a future enhancement of the LANS, ESA plans to place a reference station on the Moon in 2031, a program called NovaMoon, which will be integrated as part of the first ESA Argonaut lunar lander mission. NovaMoon will provide a lunar-based local differential, geodetic, and timing station. The primary objective of NovaMoon is to improve Moonlight's and (optionally) other LNSP navigation services, improving navigation accuracy from approximately 10 meters to the sub-meter level across the entire South Pole service area. Due to the absence of an ionosphere and troposphere on the Moon, and the high eccentricity of the LNSP node orbits above the South Pole, the degradation of differential corrections over time and distance is minimal. In these conditions, a single lunar differential station near the South Pole could provide exceptional performance to users across the entire range of South Pole latitudes, from -70 to -90 degrees. At the user level, a standardized LunaNet LANS PNT receiver, without any additional communication link or hardware modifications, should be able to process these corrections as delivered through a dedicated AFS message defined in LunaNet [2], making this approach extremely user-friendly. NovaMoon mission will have a nominal duration of 5 years. Future Argonaut missions (recurrent missions envisaged every 2-3 years) could include recurring NovaMoon payloads, ensuring a very accurate and long-term differential service provision.

This demonstration mission is expected to open up the IOC of Japan's LNSS. Successfully completing this mission enables the confirmation of its IOC-level capability and the LNSS's contribution to the LANS. JAXA is now also working on the feasibility study for the future LNSS FOC such as its further accuracy improvement, system robustness and autonomy enhancement, and service region expansion from SP region to the entire lunar surface [17]. JAXA aims to achieve the FOC before the middle of the 2030s and, together with ESA and NASA, JAXA will continue contributing to the realization of the LANS concept and the LunaNet capability for the benefit of an ecosystem for exploration and science endeavors.

References

[1] LunaNet, LunaNet Interoperability Specification, 7 February 2025, https://www.nasa.gov/directorates/somd/space-communications-navigation-program/lunanet-interoperability-specification/, (accessed 24.02.25).

[2] LunaNet Signal-In-Space Recommended Standard – Augmented Forward Signal (LSIS – AFS) Volume A, 7 February 2025, https://www.nasa.gov/wp-content/uploads/2025/02/lunanet-signal-in-space-recommended-standard-augmented-forward-signal-vol-a.pdf?emrc=0f6993, (accessed 25.02.25).

[3] Dafesh, P. A., Wong, N., Khadge, G. K., Djuknic, G., Crenshaw, J., Peters, B. C., ... & Murata, M. (2025, January). The Design of a Flexible, Interoperable Navigation Signal for Future Lunar Missions. In *Proceedings of the 2025 International Technical Meeting of The Institute of Navigation* (pp. 712-731).

[4] Dafesh, P. A., Wong, N., Khadge, G. K., Djuknic, G., Crenshaw, J., Peters, B. C., ... & Murata, M. (2024, November). The Augmented Forward Signal (AFS): Defining the Navigation Signal Standard for Future Lunar Missions. In *Inside GNSS.*

[5] International Astronomical Union. Resolution II: Resolution to establish a standard Lunar Celestial Reference System (LCRS) and Lunar Coordinate Time (TCL), XXXII International Astronomical Union General Assembly, 2024.

[6] Ashby, N.& Patla, B. , A Relativistic Framework to Estimate Clock Rates on the Moon, The Astronomical Journal, Vol 168, No 3, https://dx.doi.org/10.3847/1538-3881/ad643a, (accessed 24.02.25).

[7] Kopeikin, S. & Kaplan, G., Lunar Time In General Relativity, Physical Review D 110, October 2024. https://doi.org/10.1103/PhysRevD.110.084047 (accessed 25.02.25)

[8] M. Murata, I. Kawano, S. Kogure, Lunar Navigation Satellite System and Positioning Accuracy Evaluation, The 2022 International Technical Meeting of The Institute of Navigation, Long Beach, California, 2022, 582-586, January.
[9] M. Murata, M. Koga, Y. Nakajima, R. Yasumitsu, T. Araki, K. Makino, K. Akiyama, T. Yamamoto, K. Tanabe, S. Kogure, N. Sato, D. Toyama, K. Kitamura, K. Miyasaka, T. Kawaguchi, Y. Sato, K. Kakihara, T. Shibukawa, K. Iiyama, T. Tanaka, Lunar Navigation Satellite System: Mission, System Overview, and Demonstration, 39th International Communications Satellite Systems Conference (ICSSC 2022), Stresa, Italy, 2022, 12-15, October.
[10] NASA LCRNS, Lunar Communications Relay and Navigation Systems, https://esc.gsfc.nasa.gov/projects/LCRNS, (accessed 24.02.25).
[11] Melman, F. T., Zoccarato, P., Orgel, C., Swinden, R., Giordano, P., & Ventura-Traveset, J. (2022). LCNS positioning of a Lunar surface rover using a DEM-based altitude constraint. *Remote Sensing*, *14*(16), 3942.
[12] Audet, Y., Melman, F. T., Molli, S., Sesta, A., Plumaris, M., Psychas, D., ... & Ventura-Traveset, J. (2024). Positioning of a lunar surface rover on the south pole using LCNS and DEMs. *Advances in Space Research*, *74*(6), 2532-2550.
[13] Di Benedetto, M., Boscagli, G., De Marchi, F., Durante, D., Santi, F., Sesta, A., ... & Iess, L. (2022, September). An architecture for a lunar navigation system: orbit determination and time synchronization. In *Proceedings of the ESA's 8th International Colloquium on Scientific and Fundamental Aspects of GNSS* (pp. 14-16).
[14] Kaplan, E. D., & Hegarty, C. (Eds.). (2017). *Understanding GPS/GNSS: principles and applications*. Artech house.
[15] Artemis Requirements Document", M2M-30002 Rev A, June 2024.
[16] Positioning Error, Navipedia, 2011, https://gssc.esa.int/navipedia/index.php/Positioning_Error, (accessed 20.03.25).
[17] M. Murata, K. Akiyama, N. Satoh, Lunar Navigation Satellite System for Entire Moon Surface: HDOP and SISE Evaluation, The 2024 International Technical Meeting of The Institute of Navigation, Long Beach, California, 2024, 778-786, January. https://www.ion.org/publications/abstract.cfm?articleID=19495 (accessed 25.03.21)